



Universiteit
Leiden
The Netherlands

WWP2 confers risk to osteoarthritis by affecting cartilage matrix deposition via hypoxia associated genes

Tuerlings, M.; Janssen, G.M.C.; Boone, I.; Hoolwerff, M. van; Ruiz, A.R.; Houtman, E.; ... ; Meulenbelt, I.

Citation

Tuerlings, M., Janssen, G. M. C., Boone, I., Hoolwerff, M. van, Ruiz, A. R., Houtman, E., ... Meulenbelt, I. (2023). WWP2 confers risk to osteoarthritis by affecting cartilage matrix deposition via hypoxia associated genes. *Osteoarthritis And Cartilage*, 31(1), 39-48. doi:10.1016/j.joca.2022.09.009

Version: Publisher's Version

License: [Creative Commons CC BY 4.0 license](https://creativecommons.org/licenses/by/4.0/)

Downloaded from: <https://hdl.handle.net/1887/3513114>

Note: To cite this publication please use the final published version (if applicable).

WWP2 confers risk to osteoarthritis by affecting cartilage matrix deposition via hypoxia associated genes



M. Tuerlings †, G.M.C. Janssen ‡, I. Boone †, M. van Hoolwerff †, A. Rodriguez Ruiz †, E. Houtman †, H.E.D. Suchiman †, R.J.P. van der Wal §, R.G.H.H. Nelissen §, R. Coutinho de Almeida †, P.A. van Veelen ‡, Y.F.M. Ramos †, I. Meulenbelt †*

† Dept. of Biomedical Data Sciences, Section Molecular Epidemiology, Leiden University Medical Center, Leiden, the Netherlands

‡ Center for Proteomics and Metabolomics, Leiden University Medical Center, Leiden, the Netherlands

§ Dept. Orthopaedics, Leiden University Medical Center, Leiden, the Netherlands

ARTICLE INFO

Article history:

Received 29 June 2022

Accepted 28 September 2022

Keywords:

Osteoarthritis

WWP2

miRNA-140

Articular cartilage

SUMMARY

Objective: To explore the co-expression network of the osteoarthritis (OA) risk gene *WWP2* in articular cartilage and study cartilage characteristics when mimicking the effect of OA risk allele rs1052429-A on *WWP2* expression in a human 3D *in vitro* model of cartilage.

Method: Co-expression behavior of *WWP2* with genes expressed in lesioned OA articular cartilage ($N = 35$ samples) was explored. By applying lentiviral particle mediated *WWP2* upregulation in 3D *in vitro* pellet cultures of human primary chondrocytes ($N = 8$ donors) the effects of upregulation on cartilage matrix deposition was evaluated. Finally, we transfected primary chondrocytes with miR-140 mimics to evaluate whether miR-140 and *WWP2* are involved in similar pathways.

Results: Upon performing Spearman correlations in lesioned OA cartilage, 98 highly correlating genes ($|\rho| > 0.7$) were identified. Among these genes, we identified *GJA1*, *GDF10*, *STC2*, *WDR1*, and *WNK4*. Subsequent upregulation of *WWP2* on 3D chondrocyte pellet cultures resulted in a decreased expression of *COL2A1* and *ACAN* and an increase in *EPAS1* expression. Additionally, we observed a decreased expression of *GDF10*, *STC2*, and *GJA1*. Proteomics analysis identified 42 proteins being differentially expressed with *WWP2* upregulation, which were enriched for ubiquitin conjugating enzyme activity. Finally, upregulation of miR-140 in 2D chondrocytes resulted in significant upregulation of *WWP2* and *WDR1*.

Conclusions: Mimicking the effect of OA risk allele rs1052429-A on *WWP2* expression initiates detrimental processes in the cartilage shown by a response in hypoxia associated genes *EPAS1*, *GDF10*, and *GJA1* and a decrease in anabolic markers, *COL2A1* and *ACAN*.

© 2022 The Author(s). Published by Elsevier Ltd on behalf of Osteoarthritis Research Society International. This is an open access article under the CC BY license (<http://creativecommons.org/licenses/by/4.0/>).

* Address correspondence and reprint requests to: I. Meulenbelt, Department of Medical Statistics and Bioinformatics, Section of Molecular Epidemiology, Leiden University Medical Center, LUMC Post-zone S-05-P, PO Box 9600, 2300 RC Leiden, the Netherlands.

E-mail addresses: M.Tuerlings@lumc.nl (M. Tuerlings), G.M.C.Janssen@lumc.nl (G.M.C. Janssen), I.Boone@lumc.nl (I. Boone), M.van_Hoolwerff@lumc.nl (M. van Hoolwerff), A.Rodriguez_Ruiz@lumc.nl (A. Rodriguez Ruiz), E.Houtman@lumc.nl (E. Houtman), H.E.D.Suchiman@lumc.nl (H.E.D. Suchiman), R.J.P.van_der_Wal@lumc.nl (R.J.P. van der Wal), R.G.H.H.Nelissen@lumc.nl (R.G.H.H. Nelissen), R.Coutinho_de_Almeida@lumc.nl (R. Coutinho de Almeida), P.A.van_Veelen@lumc.nl (P.A. van Veelen), Y.F.M.Ramos@lumc.nl (Y.F.M. Ramos), i.meulenbelt@lumc.nl (I. Meulenbelt).

<https://doi.org/10.1016/j.joca.2022.09.009>

1063-4584/© 2022 The Author(s). Published by Elsevier Ltd on behalf of Osteoarthritis Research Society International. This is an open access article under the CC BY license (<http://creativecommons.org/licenses/by/4.0/>).

Introduction

Globally, osteoarthritis (OA) is a highly prevalent and disabling joint disease which confers high social and economic burden to society. Risk factors for OA include sex, abnormal joint loading, obesity, metabolic diseases, and genetic factors¹. To discover genes and underlying disease pathways, large genome wide association meta-analyses have been performed and multiple robust single nucleotide polymorphisms (SNPs) were identified significantly conferring risk to initiation and progression of OA^{2–4}. Similar to other complex traits, these risk alleles have subsequently been found to affect expression of positional genes *in cis* in disease relevant tissues, also known as allelic imbalance (AI)^{5,6}. Funded by

this mechanism, we previously used RNA sequencing data of OA articular cartilage to report on genome-wide AI expression of SNPs in cartilage specific genes, as such, providing an AI expression database to *in silico* check functional aspects of identified and/or future OA risk SNPs⁷. One of the top findings was SNP rs1052429 located in the 3'UTR of the *WWP2* gene showing highly significant AI, with risk allele rs1052429-A marking higher expression of *WWP2* relative to rs1052429-G. Among the OA risk SNPs identified in a large genome-wide meta-analysis of Icelandic and UK knee OA patients was rs34195470, located in *WWP2* gene and a proxy of our AI SNP rs1052429 ($r^2 = 0.6$)². Recently, rs34195470 was confirmed being OA risk SNP in the largest genome-wide meta-analysis so far, including individuals from 9 populations⁴. Based on these data, we could make a firm hypothesis that *WWP2*, with risk alleles rs34195470-G and rs1052429-A, confers robust risk to human OA which is marked by increased expression of *WWP2*. We also previously identified transcription of *WWP2* in cartilage being epigenetically regulated⁸, as well as being responsive in the OA pathophysiological process⁹. Moreover, *WWP2* was previously shown to be a marker for hypertrophic chondrocytes in OA knee joints¹⁰.

WWP2 is a member of the Nedd4 superfamily, a small group within the E3 ubiquitin ligase enzymes and is involved in post-translational modifications. The *WWP2* protein contains four double tryptophan (WW) domains, which allow specific protein–protein interactions and it is expressed in multiple organs throughout the body¹¹. More specifically to cartilage, Nakamura *et al.*¹² showed that *WWP2* interacts with SOX9 to form a complex that facilitates nuclear translocation of SOX9, as such enabling SOX9 transcriptional activity. Despite the association between the risk allele and higher expression levels of *WWP2* in human cartilage, the effect of *WWP2* knockout (KO) in mice with age-related and surgically induced models of OA showed that lack of *WWP2* expression resulted in increased expression of catabolic cartilage markers *RUNX2* and *ADAMTS5*¹³. In a different context, *WWP2* was found to be a host gene for microRNA-140 (miR-140), a miRNA highly expressed in cartilage and shown to be differentially expressed between preserved and lesioned OA cartilage⁹. As such, it was suggested that expression of miR-140 and the C-terminal transcript of *WWP2* (*WWP2-C*, also called *WWP2* isoform 2) are co-regulated^{14,15}.

In the current study, we set out to explore how increased levels of *WWP2*, conferring risk to OA, affect cartilage matrix. To get gain insight in the *WWP2* pathway, we started with exploring a *WWP2* co-expression network in our previous whole-transcriptome OA cartilage dataset⁹. Moreover, to study the effect of the genetic risk allele (increased levels of *WWP2*), we functionally assessed the effect of lentiviral-mediated upregulation of *WWP2* in a 3D *in vitro* model using primary human chondrocytes. Apart from conventional anabolic and catabolic cartilage markers, genes identified in the *WWP2* co-expression network were used as a read-out to evaluate the effect of *WWP2* upregulation. Since *WWP2* is involved in post-translational modifications, we explored the effect of *WWP2* upregulation on protein level by performing proteomic analysis. Finally, we explored the effects of upregulation of miR-140 in primary chondrocytes by transfection with miR-140 mimics.

Methods

Sample description

All material included in this study is obtained as part of the Research Arthritis and Articular Cartilage (RAAK) study. The RAAK-study is aimed at biobanking of joint materials of patients who underwent a total joint replacement surgery due to OA.

Classification of macroscopically preserved and lesioned OA cartilage was done as described previously¹⁶. For all sample characteristics see [Table S1](#). The RAAK-study is approved by the medical ethics committee of the Leiden University Medical Center (P08.239/P19.013).

RNA-sequencing

Lesioned OA cartilage was collected from hip and knee joints ($N = 35$ samples), snap frozen in liquid nitrogen, pulverized and homogenized in TRIzol (Invitrogen), and RNA was isolated using Qiagen RNeasy Mini Kit (Qiagen). Paired-end 2×100 bp RNA-sequencing (Illumina HiSeq2000 and Illumina HiSeq4000) was performed. Data from both Illumina platforms were integrated and analyzed with the same in-house pipeline. Additional details are described in [Supplementary methods](#).

Creating a co-expression network

We explored co-expression behavior of *WWP2* with progression of OA by correlating (Spearman correlation) *WWP2* expression levels in our RNA sequencing dataset with expression levels of all genes expressed in OA articular cartilage ($N = 20,048$ genes)⁹. To correct for multiple testing, the Benjamini-Hochberg method was used, as indicated by the false discovery rate (FDR), with a significance cutoff value of 0.05. To include the most informative genes a threshold of $|\rho| > 0.7$ and $FDR < 0.05$ were selected, corresponding to approximately the top 1% of the total significant correlations.

Lentiviral transduction

The full length *WWP2* plasmid was digested and inserted into the XhoI/XbaI sites of the pLV-CMV-IRES-eGFP lentiviral backbone (kindly provided by Prof. Dr. Hoeben). The pLV-CMV-IRES-eGFP lentiviral backbone without the *WWP2* insert was used as a control. Additional details are available in the [Supplementary methods](#).

In vitro 3D pellet cultures

3D pellet cultures were formed by adding 2.5×10^5 cells in their expansion medium to a 15 ml Falcon tube and subsequently expose them to centrifugal forces (1,200 rpm, 4 min). Chondrogenesis was initiated in serum-free chondrogenic differentiation medium. Additional details are available in the [Supplementary methods](#).

RT-qPCR

RNA was isolated from the samples using the RNeasy Mini Kit (Qiagen). cDNA synthesis was performed using the First Strand cDNA Synthesis Kit (Roche Applied Science). Subsequently, RT-qPCR was performed adjusting for housekeeping genes GAPDH and SDHA. Additional details are available in the [Supplementary methods](#).

Quantitative proteomics using TMT labeling

Lysis, digestion, TMT labeling and mass spectrometry analysis was essentially performed as described previously⁸. All searches and subsequent data analysis, including Percolator and abundance ratio calculation, were performed using Proteome Discoverer 2.4 (Thermo Scientific). Additional details are available in the [Supplementary methods](#).

Histochemistry

Sections of the 3D chondrocyte pellet culcutes were stained for glycosaminoglycan (GAG) deposition using the Alcian Blue staining. The staining was quantified using Fiji. Additional details are available in [Supplementary methods](#).

Transfection with miR-140 mimics

Primary chondrocytes were transfected with hsa-miR-3p mimic (Invitrogen) or a control mimic at 5 nM final concentration using Opti-MEM (Gibco) and Lipofectamine RNAiMax Transfection reagent (Invitrogen) according to manufacturer's protocol. Additional details are available in [Supplementary methods](#).

An overview of the applied strategy can be seen in [Fig. 1](#). The RNA sequencing data of the articular cartilage is deposited at ArrayExpress (E-MTAB-7313). Further data generated and used in this study is not openly available due to reasons of sensitivity and are available from the corresponding author upon reasonable request.

Results

Co-expression network of WWP2

To identify genes that are regulated by, or co-expressed with, WWP2 in OA cartilage, we used RNA sequencing data of lesioned OA cartilage [$N = 35$ samples, [Table S1\(A\)](#)] to perform Spearman correlation between expression levels of WWP2 and genes expressed in cartilage [$N = 20,048$ genes, [Table S2](#), [Fig. 1\(A\)](#)]. We identified 98 genes highly correlating ($|\rho| > 0.7$) to WWP2. These 98 genes were significantly enriched for, amongst others, GO-terms Extracellular exosome (GO:0070062, 36 genes), characterized by expression of

GJA1 (encoding gap junction alpha 1), *SMO* (encoding smoothed frizzled class receptor), and *WDR1* (encoding WD repeat domain 1), and Myelin sheath (GO:0043209, 10 genes), characterized by expression of *WDR1*, *RALA* (encoding RAS like proto-oncogene A), and *CCT5* (encoding chaperonin containing TCP1 subunit 5) ([Table S3](#)). As shown in [Fig. S1](#), genes highly correlating to WWP2 ($N = 98$) formed a highly interconnected network, i.e., genes that are all highly correlating with each other. In this network we identified direct and indirect relations with WWP2, including *GJA1* ($\rho = -0.81$, 70 connections, i.e., highly correlating to 70 genes in the network), *WNK4* (encoding WNK lysine deficient protein kinase 4, $\rho = 0.81$, 37 connections), *ACAN* (encoding aggrecan, $\rho = 0.78$, 16 connections), and *STC2* (encoding stanniocalcin 2, $\rho = 0.77$, 17 connections).

Lentiviral particle-mediated upregulation of WWP2

The effect of upregulation of WWP2 was studied on cartilaginous matrix deposition in *in vitro* 3D chondrocyte pellet cultures, by creating a lentiviral particle mediated upregulation of WWP2. 3D pellet cultures were harvested after three or seven days of culturing and gene ($N = 16$ pellet cultures of $N = 8$ donors) and protein ($N = 16$ pellet cultures of $N = 4$ donors) expression levels were measured [[Table S1\(B\)](#)]. First, we confirmed whether WWP2 upregulation was successful by measuring both gene and protein expression levels at day zero of the 3D chondrocyte pellet culture, and we observed a significant increase in WWP2 gene expression levels [$P = 1.0 \times 10^{-5}$, [Figs. S2\(A\)–\(B\)](#)], which was confirmed on protein level [$P = 3.2 \times 10^{-6}$, [Fig. S2\(C\)](#)].

Effect of WWP2 upregulation on cartilage matrix deposition

Next, we evaluated effect of WWP2 upregulation on expression levels of conventional cartilage genes during 3D pellet culture of

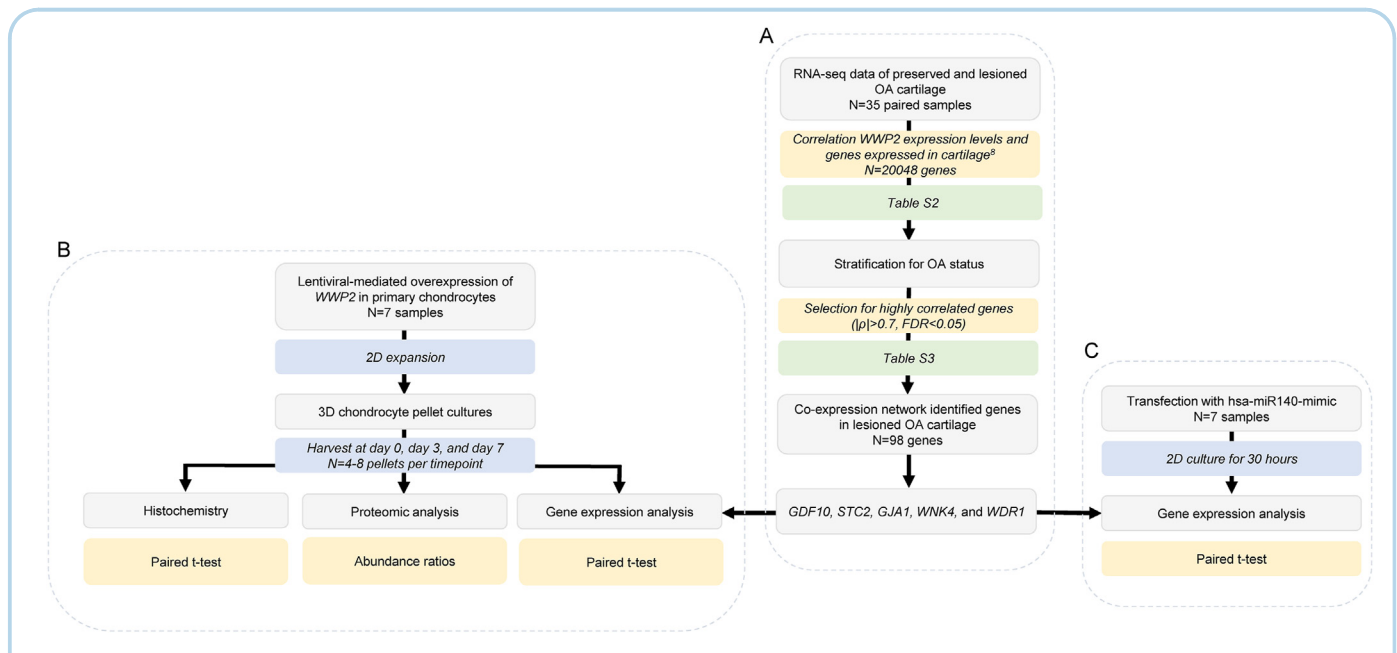


Fig. 1

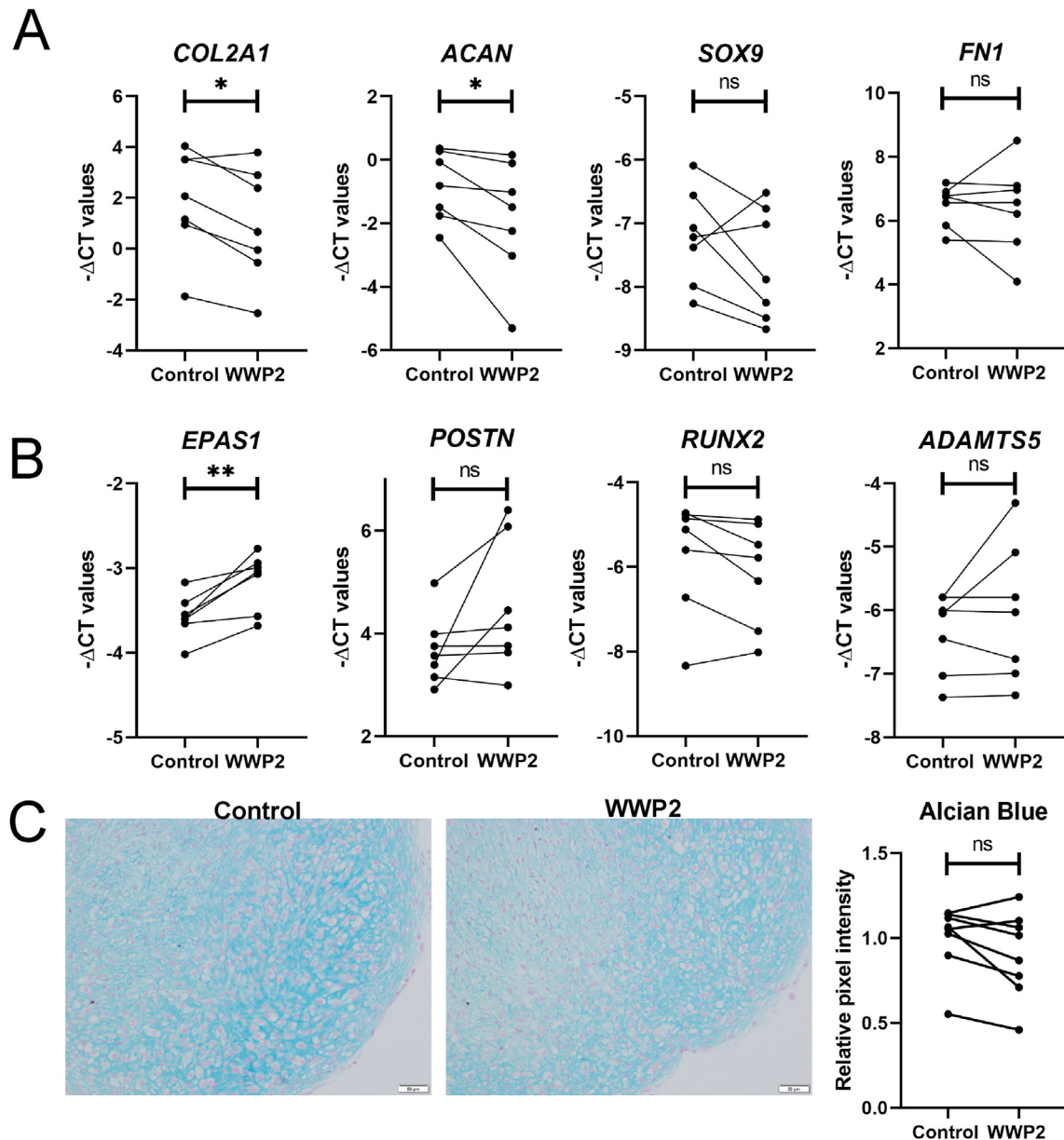


Fig. 2

mRNA expression levels of cartilage matrix markers (A) and cartilage degeneration markers (B) for pellets with WWP2 upregulation and their controls at day 7 ($N = 11-12$ pellet cultures, $N = 7$ donors). (C) Alcian Blue staining visualizing GAGs deposition in WWP2 overexpressed pellets and their controls after 7 days of culturing ($N = 26$ pellet cultures, $N = 8$ donors). The scale bar indicates 50 μm . Ns: not significant, $*P < 0.05$, $**P < 0.005$ upon performing a Paired sample t -test.

seven days [Fig. 1(B)]. As shown in Fig. 2(A), we found significant reduced gene expression of *ACAN* ($FC = 0.80$, $P = 0.04$) and *COL2A1* (encoding collagen type 2 alpha chain 1, $FC = 0.77$, $P = 0.01$), in WWP2 upregulated pellets compared to their controls at day seven (Table S4). Moreover, we showed significant increased gene expression of degeneration markers *EPAS1* (encoding endothelial PAS domain protein 1, $FC = 1.56$, $P = 0.004$) [Fig. 2(B)]. Notably, *SOX9*, *ADAMTS5* and *RUNX2*, which were previously linked to WWP2 function, were not consistently changed upon WWP2

upregulation. Moreover, we stained 3D pellet cultures for presence of glycosaminoglycans (GAGs) using Alcian Blue staining, and observed a trend towards decreased Alcian Blue intensity when comparing WWP2 upregulated pellets with controls [Fig. 2(C)].

Effect of WWP2 upregulation on genes correlated to WWP2

To investigate functional relationships between WWP2 and identified correlating and highly interconnected genes, we selected

GDF10 (encoding growth differentiation factor 10, $\rho = 0.72$, 18 connections), *STC2* ($\rho = 0.77$, 17 connections), *GJA1* ($\rho = -0.81$, 70 connections), *WDR1* (encoding WD repeat-containing protein 1, $\rho = -0.70$, 5 connections), and *WNK4* ($\rho = 0.81$, 37 connections) from the network (Fig. 1) to use as read-out of *WWP2* upregulation in 3D chondrocyte pellet cultures [Fig. 1(B)]. As shown in Fig. 3, we observed significant decreased gene expression of *GDF10* (FC = 0.62, $P = 0.002$) and *STC2* (FC = 0.73, $P = 0.04$) with upregulation of *WWP2*. Albeit not significant, gene expression of *GJA1* (FC = 0.76, $P = 0.08$) was also consistently lower in *WWP2* upregulated pellets. Together, these data suggest that *GDF10*, *STC2*, and *GJA1* are downstream of *WWP2* either by direct or indirect activity. In contrast, *WNK4* and *WDR1* did not show consistent changes in expression with upregulation of *WWP2*, suggesting *WNK4* and *WDR1* are rather upstream in the pathway of *WWP2*.

Proteomics

To study the extent to which gene expression levels translate to protein levels, we performed proteomics analysis. Prior to differential expression analysis of pellet cultures with and without *WWP2* upregulation, we explored protein expression levels of cartilage markers in our control pellet cultures at day three and day seven of 3D pellet culture. Upon comparing day three and day seven with day zero of control pellets, we observed increased protein expression of cartilage markers COL2A1 (FC = 2.68 and FC = 32.94, respectively), ACAN (FC = 5.28 and FC = 13.75, respectively), COMP (cartilage oligomeric matrix protein, FC = 5.31 and FC = 20.25, respectively), and FN1 (fibronectin, FC = 2.12 and FC = 3.51, respectively) (Table S5, Fig. S3). Moreover, mesenchymal markers CD44 (FC = 0.83 and FC = 0.46, respectively) and CD166 (FC = 0.79 and FC = 0.62, respectively) and IGFBP3 (insulin growth factor binding protein 3, FC = 0.10 and FC = 0.10, respectively) were downregulated on both days. Together, this indicates that cartilage-like matrix is produced by chondrocytes already at day three, but is increasing towards day seven. Notably, SOX9 was not detected in the proteomics analysis.

Next, we evaluated the effect of *WWP2* upregulation on cartilage matrix deposition on protein level [Fig. 1(B)]. Since we observed increased protein expression of cartilage markers in control pellet cultures already on day three [Fig. S3(A)], we pooled day three and day seven for further analysis to increase power.

Upon comparing pellet cultures with and without *WWP2* upregulation, we found *WWP2* still being significantly upregulated after three and seven days of culturing. Furthermore, we found 42 proteins significantly differentially expressed [Fig. 4(A), Table S6], of which *GJA1* (FC = 0.54) was most significantly downregulated in *WWP2* upregulated pellet cultures, confirming the downregulation observed on gene expression level (FC = 0.76). Oppositely, the observed changes in *ACAN* and *COL2A1* gene expression levels were not confirmed on protein level. Proteins encoded by *SOX9*, *EPAS1*, *RUNX2*, and *ADAMTS5* were either not identified or did not show unique peptides. Upon performing enrichment analysis on the 42 differentially expressed proteins, we found significant enrichment for ubiquitin conjugating enzyme activity (5 proteins, FDR = 0.002) and ubiquitin-protein transferase activity (6 proteins, FDR = 0.03), both terms characterized by expression of, amongst others, *UBE2D4*, *UBE2L3*, and *UBE2D1*. Furthermore, these 42 proteins showed significant protein–protein interactions [$P = 0.02$, Fig. 4(B)], also representing ubiquitin conjugating enzyme activity.

miR-140-3p and *WWP2*

Since it has been suggested that *WWP2* and miR-140 are co-expressed^{14,15}, we transfected primary chondrocytes with miR-140-3p mimics, to assess whether this miRNA regulates *WWP2* expression or similar genes as involved in the *WWP2* co-expression network [$N = 7$, Table S1(B), Fig. 1(C)]. To investigate whether miR-140-3p regulates *WWP2*, we first evaluated the effects of miR-140-3p mimic on expression levels of *WWP2* full length and *WWP2* splice variants isoform 2, isoform 4, and isoform 6 (Fig. S4). MiR-140 is suggested to be co-expressed with splice variant *WWP2* isoform 2, also called *WWP2-C*, as they share the promoter¹⁵. Isoform 4 is also known as *WWP2-N* and is a transcript that does not contain miR-140 (Fig. S4). As shown in Fig. 5(A), we observed significant increased expression levels of *WWP2* (FC = 1.22, $P = 0.02$) with upregulation of miR-140-3p. Moreover, we observed consistent increased expression of *WWP2* isoform 6 (FC = 1.29, $P = 0.06$), while significant decreased expression of isoform 4 (FC = 0.63, $P = 0.02$) (Table S7). Notably, we did not see effect on expression levels of *WWP2* isoform 2, also called *WWP2-C*. With respect to highly correlated genes, we observed increased expression of *WDR1* (FC = 1.79, $P = 1.00 \times 10^{-3}$), one of the genes that was not consistently changed with *WWP2* upregulation [Fig. 5(B)]. Albeit

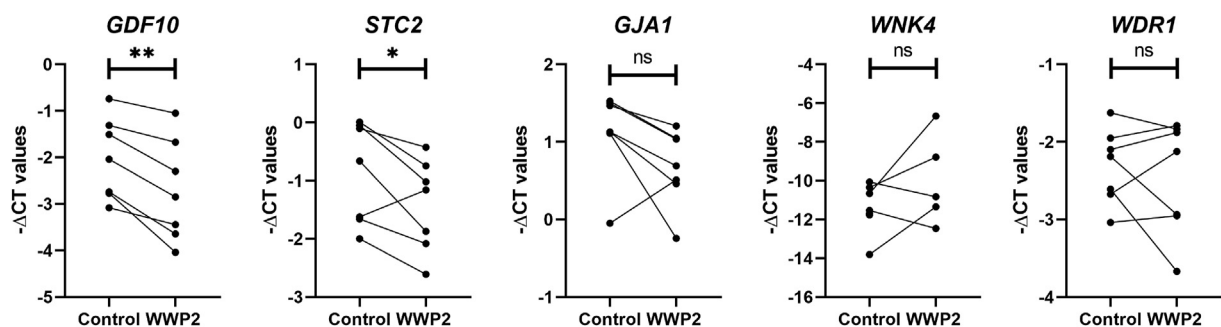


Fig. 3

mRNA expression levels of genes correlating with *WWP2* in *WWP2* upregulated 3D chondrocyte pellet cultures compared to their controls after 7 days of culturing ($N = 6–12$ pellet cultures, $N = 7$ donors). Ns: not significant, $*P < 0.05$, $**P < 0.05$ upon performing a Paired sample *t*-test.

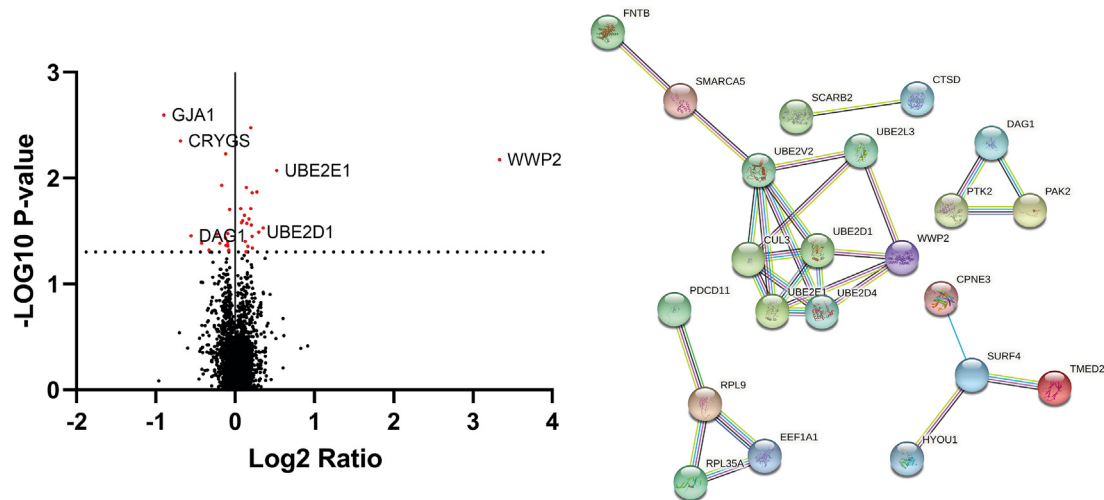


Fig. 4

Osteoarthritis and Cartilage

(A) Volcano plot of proteins differentially expressed between WWP2 transduced 3D pellet cultures and their controls at day three and day seven together ($N = 16$ pellets, $N = 4$ donors). The red dots indicate the significantly differentially expressed proteins. (B) Protein–protein interaction network in STRING.

not significant, we observed an increased expression of *STC2* ($FC = 1.55$, $P = 0.08$), which is also contradictory to the effects of *WWP2* upregulation. Moreover, we did not observe consistent effects on *GJA1* expression levels.

Discussion

By combining a genome-wide screen for cartilage specific *AI7* and large scale GWAS^{2,4}, we hypothesized that upregulated expression of *WWP2* confers robust risk to OA. Here, we set out to functionally investigate the role of *WWP2* in cartilage by exploring the *WWP2* co-expression network in a previously assessed RNA sequencing dataset⁹. Moreover, lentiviral-mediated upregulation of *WWP2* was shown to have detrimental effects on cartilage matrix deposition, as shown by downregulation of *COL2A1* and *ACAN* and upregulation of *EPAS1*. Apart from conventional anabolic and catabolic cartilage markers, genes identified in the *WWP2* co-expression network were used as read-out, showing *GDF10*, *STC2*, and *GJA1* being responsive to *WWP2* upregulation. Furthermore, to explore effects of miR-140-3p, that was suggested to be co-regulated with *WWP2*, we transfected primary chondrocytes with miR-140-3p mimics.

Based on *AI* expression of the OA risk SNP rs1052429, we hypothesized that *WWP2* confers risk to OA onset by upregulated expression, whereas *WWP2* exhibited FDR significantly lower expression in lesioned compared to preserved cartilage ($FC = 0.78$, $FDR = 5.3 \times 10^{-3}$), together suggesting that lower expression levels of *WWP2* in lesioned OA cartilage are rather an attempt of chondrocytes to reverse the OA state than a cause to the OA process^{17,18}. Concomitantly, co-expression network analyses showed 98 highly and significantly ($|\rho| > 0.7$, $FDR < 0.05$) correlating genes to *WWP2*, including *GJA1* ($\rho = -0.81$), *WNK4* ($\rho = 0.81$), *ACAN* ($\rho = 0.78$), and *STC2* ($\rho = 0.77$) (Table S2). Previously, it was shown that *WWP2* interacts with *SOX9* and that it regulates *SOX9* transcriptional activity¹². Although *SOX9* is highly expressed in cartilage, *SOX9* was

not among the high and significant correlations ($\rho = 0.5$). On the other hand, *SOX9* was previously shown to regulate the expression of, amongst others *ACAN*^{19,20}, which was here shown to be highly correlated to *WWP2* ($\rho = 0.78$).

Upon studying the effect of upregulation of *WWP2*, we found *EPAS1* and *GDF10* being genes that had most consistent and significant changed levels of gene expression. *EPAS1*, encoding hypoxia-inducible factor 2 alpha, is known for its role in endochondral ossification and is a known cartilage degradation marker in OA^{21,22}. *GDF10*, also known as bone morphogenic protein 3, is involved in osteogenesis as it inhibits osteoblast differentiation via *SMAD2* and *SMAD3*^{18,23}. The latter also being previously identified as OA susceptibility gene². Furthermore, lower expression level of *GDF10* was associated with OA severity in both bone and cartilage²⁴. Interestingly, *GDF10* was shown to be a hypoxia inducible gene, like *EPAS1*, which is regulated by *SOX9* and was identified as marker for differentiated chondrocytes as it inhibits adipogenesis and osteogenesis²⁵. Both *EPAS1* and *GDF10* were not in the proteomics analysis, either because they were not measured (*EPAS1*) or they did not show unique peptides (*GDF10*). Additionally, we observed a decrease in *STC2* and *GJA1* expression. Downregulation of *GJA1* did not reach statistical significance on gene expression level, while on protein level *GJA1* was the most significantly downregulated protein. *STC2* is a glycoprotein and upregulation of *STC2* in mice has been shown to delay endochondral ossification^{26,27}. Moreover, it was shown that *STC2* was higher expressed in healthy cartilage compared to osteophytic cartilage²⁸, suggesting its potential role in initiation and progression of OA in presence of higher *WWP2* expression. *GJA1*, also known as connexin 43, is a major protein of functional gap junctions which allows for cell–cell communication. More specific to cartilage, connexin 43 is essential in mechano-transduction²⁹. Alterations in connexin 43 expression and localization affects this cell–cell communication, by which homeostasis to maintain cartilage tissue gets disturbed³⁰. Notably, like *EPAS1* and *GDF10*, the function of connexin 43 is regulated by oxygen

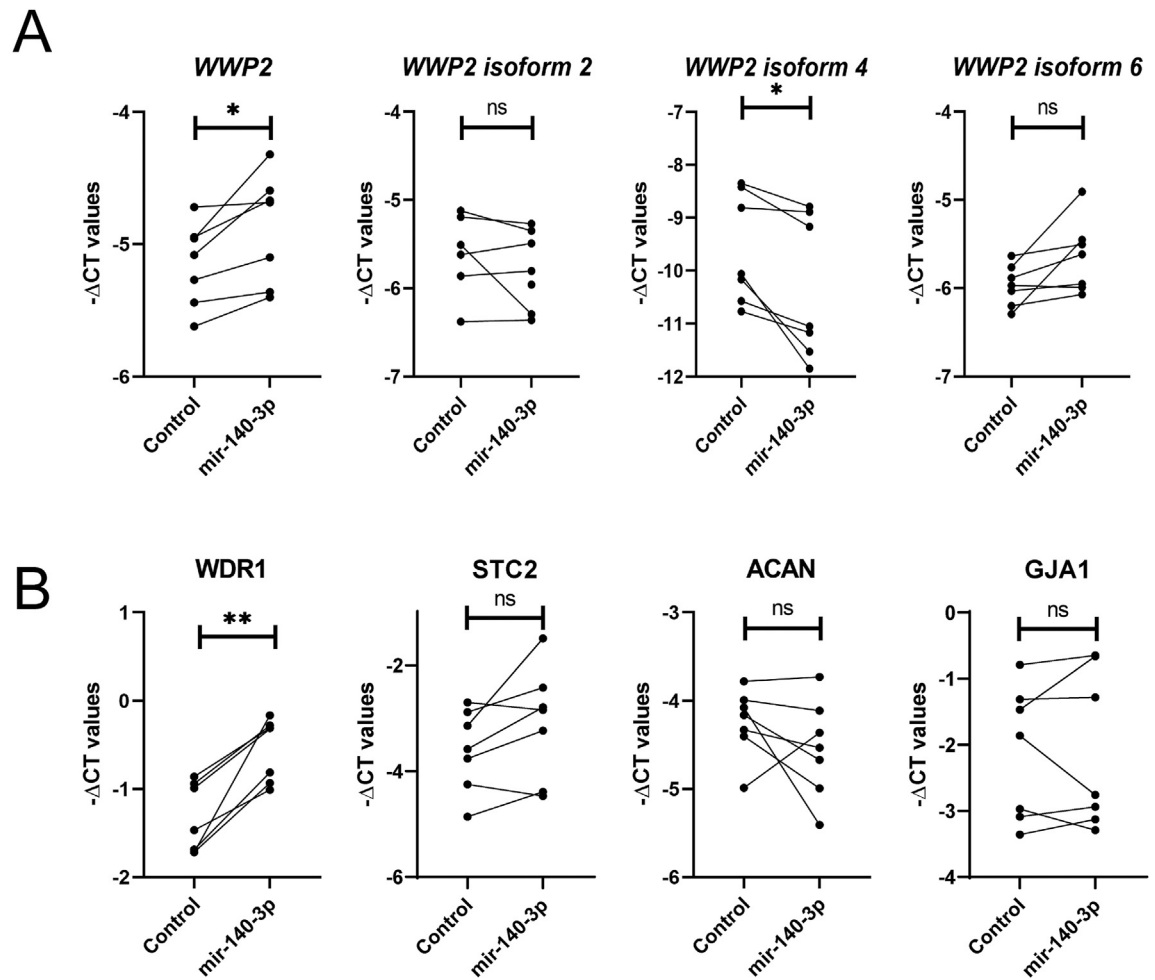


Fig. 5

mRNA expression levels upon transfection with miR-140-3p. (A) expression levels of WWP2 and its isoforms. (B) Expression levels of genes correlated to WWP2 ($N = 8$ wells, $N = 4$ donors). Ns: not significant, $*P < 0.05$, $**P < 0.005$ upon performing a Paired sample t -test.

levels³¹. Upregulation of *EPAS1* and downregulation of *GDF10*, *STC2* and *GJA1* suggests that increased level of WWP2 has detrimental effects on cartilage matrix deposition, which acts via hypoxia associated chondrocyte dedifferentiation. This is in line with decreased gene expression levels of *COL2A1* and *ACAN*, two major cartilage markers.

To evaluate the effects of WWP2 upregulation on cartilage matrix deposition on protein level, we performed proteomics analysis. We did confirm upregulation of WWP2 on day zero, which was still present at day three and seven (Fig. 4, Fig. S2). Moreover, we found 42 significantly differentially expressed proteins upon comparing pellet cultures with and without WWP2 upregulation, of which *GJA1* was most significantly differentially expressed and showing the highest fold change ($FC = 0.49$). The observed differences in gene expression levels of *COL2A1* and *ACAN* with WWP2 upregulation were not observed on protein level (Table S6), which might be due to the relatively low sample size ($N = 4$ donors) or due to suboptimal timepoint chosen to evaluate the effect of WWP2 on either gene or protein expression level. Since WWP2 is a E3

ubiquitin ligase and the differentially expressed proteins were significantly enriched for ubiquitin conjugating enzyme activity and ubiquitin-protein transferase activity, upregulation of WWP2 could also affect proteins cellular location, activity, and protein-protein interactions without changing expression levels itself, which is not captured by our read-outs. Moreover, it should be noted that the here observed fold differences were relatively low and additional validation and replication are necessary.

Since it has been suggested that miR-140 is co-expressed with *WWP2-C¹⁴*, *WWP2* isoform 2, we generated upregulation of miR-140 in 2D primary chondrocytes to explore whether *WWP2* and miR-140 are involved in similar pathways. In the miR-140 upregulated cells, we observed significant increased expression levels of *WWP2*, indicating miR-140 indeed targets *WWP2*. Nonetheless, given the predicted *WWP2* target site of miR-140 (3'UTR of *WWP2* isoform 6³²) and the absence of SNPs in this region in linkage disequilibrium with the OA risk SNP rs1052429, the genetic *WWP2* risk nor the AI is brought about via an aberrant miR-140 binding to *WWP2*. The fact that we did not observe consistent changes in

expression levels of *WWP2* isoform 2> suggests that *WWP2* isoform 2 and miR-140 indeed share the intron 10 (*WWP2* full length) promotor as hypothesized previously by Rice *et al.*¹⁵. Additional research is required to fully understand the role of miR-140 in the *WWP2* pathway and in OA pathophysiology in general.

Although lower expression of *WWP2* was observed in lesioned compared to preserved cartilage in our previous study⁹, genetic evidence suggests that higher expression of *WWP2* predisposes to development of OA, indicating that downregulation in OA pathophysiology is merely a response to the pathophysiological process and a beneficial attempt of chondrocytes to reverse the OA state⁷. The latter shows that genes identified being differentially expressed between preserved and lesioned OA articular cartilage are a response to the OA pathophysiological process and not necessarily causal to the OA pathophysiological process. To identify genes causal to OA, genetic studies have to be performed. To our surprise, Styrkarsdottir *et al.*² reported on *WWP2* expression in adipose tissue as function of SNP rs4985453-G, a proxy of their identified OA risk allele rs34195470-G ($R^2 = 0.79$) and our AI SNP rs1052429-A ($R^2 = 0.77$), highlighting the OA risk allele being associated with lower expression levels of *WWP2*. Upon investigating the GTEx eQTL data of *WWP2* with the highlighted SNPs³³, we found only data showing consistently higher expression of *WWP2* as function of OA risk alleles of the respective SNPs across multiple tissues (Fig. S5), underscoring the aberrant effects observed here with *WWP2* upregulation. Although Mokuda *et al.*¹³ showed that lack of *WWP2* expression in mice resulted in increased expression of *RUNX2* and *ADAMTS5*, we here did not observe consistent changes in expression of *RUNX2* or *ADAMTS5* upon upregulation of *WWP2* in our human chondrocyte pellet cultures and culturing for seven days. This difference could be due to translational limitations from mice to humans. Alternatively, we here create neocartilage, and the effect on *RUNX2* and *ADAMTS5* may be a temporal or time-dependent effect, which we do not observe at day seven of culturing.

In conclusion, our data provide support to our hypothesis that high levels of *WWP2* have detrimental effects on cartilage homeostasis. We identified *EPAS1*, *GJA1*, *GDF10*, and *STC2*, all genes involved in chondrocyte dedifferentiation, to be involved in the *WWP2* pathway. Moreover, we showed that miR-140 is likely involved in similar pathways as *WWP2* and miR-140 might play a role in regulating *WWP2* expression. Together these data contribute to a better understanding of how *WWP2* confers risk to OA and is a step towards translation from bench to bedside.

Data availability

The RNA sequencing data of the articular cartilage is deposited at ArrayExpress (E-MTAB-7313). Further data generated and used in this study is not openly available due to reasons of sensitivity and are available from the corresponding author upon reasonable request.

Contributions

All authors contributed to the study conception and design. Material preparation, data collection and analysis were performed by M. Tuerlings, G.M.C. Janssen, P.A. van Veelen, Y.F.M. Ramos, and I. Meulenbelt. The first draft of the manuscript was written by M. Tuerlings, Y.F.M. Ramos, and I. Meulenbelt and all authors commented on previous versions of the manuscript. All authors read and approved the final manuscript.

Competing interests

The authors have no relevant financial or non-financial interests to disclose.

Funding

The study was funded by the Dutch Scientific Research council NWO/ZonMW VICI scheme (nr 91816631/528), Dutch Arthritis Society (DAA_10_1-402), BBMRI-NL complementation project (CP2013-83), European Commission Seventh Framework programme (TreatOA, 200800), and Ana fonds (O2015-27).

Acknowledgments

We thank all the participants of the RAAK study. The LUMC has and is supporting the RAAK study. We thank all the members of our group for valuable discussion and feedback. We also thank Enrike van der Linden, Demiën Broekhuis, Peter van Schie, Shaho Hasan, Maartje Meijer, Daisy Latijnhouwers, Anika Rabelink-Hoogenstraaten, and Geert Spierenburg for collecting the RAAK material. We thank the Sequence Analysis Support Core (SASC) of the Leiden University Medical Center for their support. The study was funded by the Dutch Scientific Research council NWO/ZonMW VICI scheme (nr 91816631/528), Dutch Arthritis Society (DAA_10_1-402), BBMRI-NL complementation project (CP2013-83), European Commission Seventh Framework programme (TreatOA, 200800), and Ana fonds (O2015-27). Data is generated within the scope of the Medical Delta programs Regenerative Medicine 4D: Generating complex tissues with stem cells and printing technology and Improving Mobility with Technology.

Supplementary data

Supplementary data to this article can be found online at <https://doi.org/10.1016/j.joca.2022.09.009>.

References

- Vina ER, Kwoh CK. Epidemiology of osteoarthritis: literature update. *Curr Opin Rheumatol* 2018;30(2):160–7, <https://doi.org/10.1097/bor.0000000000000479> [published Online First: 2017/12/12].
- Styrkarsdottir U, Lund SH, Thorleifsson G, Zink F, Stefansson OA, Sigurdsson JK, *et al.* Meta-analysis of Icelandic and UK data sets identifies missense variants in *SMO*, *IL11*, *COL11A1* and 13 more new loci associated with osteoarthritis. *Nat Genet* 2018;50(12):1681–7, <https://doi.org/10.1038/s41588-018-0247-0> [published Online First: 2018/10/31].
- Zengini E, Hatzikotoulas K, Tachmazidou I, Steinberg J, Hartwig FP, Southam L, *et al.* Genome-wide analyses using UK Biobank data provide insights into the genetic architecture of osteoarthritis. *Nat Genet* 2018;50(4):549–58, <https://doi.org/10.1038/s41588-018-0079-y> [published Online First: 2018/03/22].
- Boer CG, Hatzikotoulas K, Southam L, Stefánsdóttir L, Zhang Y, Coutinho de Almeida R, *et al.* Deciphering osteoarthritis genetics across 826,690 individuals from 9 populations. *Cell* 2021, <https://doi.org/10.1016/j.cell.2021.07.038> [published Online First: 2021/08/28].
- Gee F, Clubbs CF, Raine EV, Reynard LN, Loughlin J. Allelic expression analysis of the osteoarthritis susceptibility locus that maps to chromosome 3p21 reveals cis-acting eQTLs at *GNL3* and *SPCS1*. *BMC Med Genet* 2014;15:53, <https://doi.org/10.1186/1471-2350-15-53> [published Online First: 2014/06/03].
- Raine EV, Dodd AW, Reynard LN, Loughlin J. Allelic expression analysis of the osteoarthritis susceptibility gene *COL11A1* in human joint tissues. *BMC Musculoskelet Disord* 2013;14:85, <https://doi.org/10.1186/1471-2474-14-85> [published Online First: 2013/03/19].

7. den Hollander W, Pulyakhina I, Boer C, Bomer N, van der Breggen R, Arindrarto W, *et al.* Annotating transcriptional effects of genetic variants in disease-relevant tissue: transcriptome-wide allelic imbalance in osteoarthritic cartilage. *Arthritis Rheumatol* 2019;71(4):561–70, <https://doi.org/10.1002/art.40748> [published Online First: 2018/10/10].
8. den Hollander W, Ramos YF, Bomer N, Elzinga S, van der Breggen R, Lakenberg N, *et al.* Transcriptional associations of osteoarthritis-mediated loss of epigenetic control in articular cartilage. *Arthritis Rheumatol* 2015;67(8):2108–16, <https://doi.org/10.1002/art.39162> [published Online First: 2015/04/22].
9. Coutinho de Almeida R, Ramos YFM, Mahfouz A, den Hollander W, Lakenberg N, Houtman E, *et al.* RNA sequencing data integration reveals an miRNA interactome of osteoarthritis cartilage. *Ann Rheum Dis* 2019;78(2):270–7, <https://doi.org/10.1136/annrheumdis-2018-213882> [published Online First: 2018/12/07].
10. Ji Q, Zheng Y, Zhang G, Hu Y, Fan X, Hou Y, *et al.* Single-cell RNA-seq analysis reveals the progression of human osteoarthritis. *Ann Rheum Dis* 2019;78(1):100–10, <https://doi.org/10.1136/annrheumdis-2017-212863>.
11. Chantry A. WWP2 ubiquitin ligase and its isoforms: new biological insight and promising disease targets. *Cell Cycle* 2011;10(15):2437–9, <https://doi.org/10.4161/cc.10.15.16874> [published Online First: 2011/07/14].
12. Nakamura Y, Yamamoto K, He X, Otsuki B, Kim Y, Murao H, *et al.* Wwp2 is essential for palatogenesis mediated by the interaction between Sox9 and mediator subunit 25. *Nat Commun* 2011;2:251, <https://doi.org/10.1038/ncomms1242> [published Online First: 2011/03/24].
13. Mokuada S, Nakamichi R, Matsuzaki T, Ito Y, Sato T, Miyata K, *et al.* Wwp2 maintains cartilage homeostasis through regulation of Adamts5. *Nat Commun* 2019;10(1):2429, <https://doi.org/10.1038/s41467-019-10177-1>.
14. Yang J, Qin S, Yi C, Ma G, Zhu H, Zhou W, *et al.* MiR-140 is co-expressed with Wwp2-C transcript and activated by Sox9 to target Sp1 in maintaining the chondrocyte proliferation. *FEBS Lett* 2011;585(19):2992–7, <https://doi.org/10.1016/j.febslet.2011.08.013> [published Online First: 2011/08/30].
15. Rice SJ, Beier F, Young DA, Loughlin J. Interplay between genetics and epigenetics in osteoarthritis. *Nat Rev Rheumatol* 2020;16(5):268–81, <https://doi.org/10.1038/s41584-020-0407-3>.
16. Ramos YF, den Hollander W, Bovee JV, Bomer N, van der Breggen R, Lakenberg N, *et al.* Genes involved in the osteoarthritis process identified through genome wide expression analysis in articular cartilage; the RAAK study. *PLoS One* 2014;9(7), e103056, <https://doi.org/10.1371/journal.pone.0103056> [published Online First: 2014/07/24].
17. Reynard LN. Analysis of genetics and DNA methylation in osteoarthritis: what have we learnt about the disease? *Semin Cell Dev Biol* 2017;62:57–66, <https://doi.org/10.1016/j.semcdb.2016.04.017> [published Online First: 2016/05/01].
18. Rice SJ, Cheung K, Reynard LN, Loughlin J. Discovery and analysis of methylation quantitative trait loci (mQTLs) mapping to novel osteoarthritis genetic risk signals. *Osteoarthritis Cartilage* 2019;27(10):1545–56, <https://doi.org/10.1016/j.joca.2019.05.017> [published Online First: 2019/06/08].
19. Sekiya I, Tsuji K, Koopman P, Watanabe H, Yamada Y, Shinomiya K, *et al.* SOX9 enhances aggrecan gene promoter/enhancer activity and is up-regulated by retinoic acid in a cartilage-derived cell line, TC6. *J Biol Chem* 2000;275(15):10738–44, <https://doi.org/10.1074/jbc.275.15.10738> [published Online First: 2001/02/07].
20. Nishimura R, Hata K, Takahata Y, Murakami T, Nakamura E, Yagi H. Regulation of cartilage development and diseases by transcription factors. *J Bone Metab* 2017;24(3):147–53, <https://doi.org/10.11005/jbm.2017.24.3.147> [published Online First: 2017/09/29].
21. Yang S, Kim J, Ryu JH, Oh H, Chun CH, Kim BJ, *et al.* Hypoxia-inducible factor-2alpha is a catabolic regulator of osteoarthritic cartilage destruction. *Nat Med* 2010;16(6):687–93, <https://doi.org/10.1038/nm.2153> [published Online First: 2010/05/25].
22. Saito T, Fukai A, Mabuchi A, Ikeda T, Yano F, Ohba S, *et al.* Transcriptional regulation of endochondral ossification by HIF-2alpha during skeletal growth and osteoarthritis development. *Nat Med* 2010;16(6):678–86, <https://doi.org/10.1038/nm.2146> [published Online First: 2010/05/25].
23. Matsumoto Y, Otsuka F, Hino J, Miyoshi T, Takano M, Miyazato M, *et al.* Bone morphogenetic protein-3b (BMP-3b) inhibits osteoblast differentiation via Smad2/3 pathway by counteracting Smad1/5/8 signaling. *Mol Cell Endocrinol* 2012;350(1):78–86, <https://doi.org/10.1016/j.mce.2011.11.023> [published Online First: 2011/12/14].
24. Chou CH, Lee CH, Lu LS, Song IW, Chuang HP, Kuo SY, *et al.* Direct assessment of articular cartilage and underlying subchondral bone reveals a progressive gene expression change in human osteoarthritic knees. *Osteoarthritis Cartilage* 2013;21(3):450–61, <https://doi.org/10.1016/j.joca.2012.11.016> [published Online First: 2012/12/12].
25. Lafont JE, Talma S, Hopfgarten C, Murphy CL. Hypoxia promotes the differentiated human articular chondrocyte phenotype through SOX9-dependent and -independent pathways. *J Biol Chem* 2008;283(8):4778–86, <https://doi.org/10.1074/jbc.M707729200> [published Online First: 2007/12/14].
26. Gagliardi AD, Kuo EY, Raulic S, Wagner GF, DiMattia GE. Human stanniocalcin-2 exhibits potent growth-suppressive properties in transgenic mice independently of growth hormone and IGFs. *Am J Physiol Endocrinol Metab* 2005;288(1):E92–E105, <https://doi.org/10.1152/ajpendo.00268.2004> [published Online First: 2004/09/16].
27. Chang AC, Hook J, Lemckert FA, McDonald MM, Nguyen MA, Hardeman EC, *et al.* The murine stanniocalcin 2 gene is a negative regulator of postnatal growth. *Endocrinology* 2008;149(5):2403–10, <https://doi.org/10.1210/en.2007-1219> [published Online First: 2008/02/09].
28. Gelse K, Ekici AB, Cipa F, Swoboda B, Carl HD, Olk A, *et al.* Molecular differentiation between osteophytic and articular cartilage—clues for a transient and permanent chondrocyte phenotype. *Osteoarthritis Cartilage* 2012;20(2):162–71, <https://doi.org/10.1016/j.joca.2011.12.004> [published Online First: 2012/01/03].
29. Gago-Fuentes R, Bechberger JF, Varela-Eirin M, Varela-Vazquez A, Acea B, Fonseca E, *et al.* The C-terminal domain of connexin43 modulates cartilage structure via chondrocyte phenotypic changes. *Oncotarget* 2016;7(45):73055–67, <https://doi.org/10.18632/oncotarget.12197> [published Online First: 2016/09/30].
30. Mayan MD, Gago-Fuentes R, Carpintero-Fernandez P, Fernandez-Puente P, Filgueira-Fernandez P, Goyanes N, *et al.* Articular chondrocyte network mediated by gap junctions: role in metabolic cartilage homeostasis. *Ann Rheum Dis* 2015;74(1):275–84, <https://doi.org/10.1136/annrheumdis-2013-204244> [published Online First: 2013/11/15].
31. Knight MM, McGlashan SR, Garcia M, Jensen CG, Poole CA. Articular chondrocytes express connexin 43 hemichannels and P2 receptors - a putative mechanoreceptor complex involving the primary cilium? *J Anat* 2009;214(2):275–83, <https://doi.org/10.1111/j.1365-3113.2008.04444.x>

- doi.org/10.1111/j.1469-7580.2008.01021.x [published Online First: 2009/02/12].
32. Agarwal V, Bell GW, Nam J-W, Bartel DP. Predicting effective microRNA target sites in mammalian mRNAs. *Elife* 2015;4, e05005, <https://doi.org/10.7554/eLife.05005>.
33. The Genotype-Tissue Expression (GTEx) project. *Nat Genet* 2013;45(6):580–5, <https://doi.org/10.1038/ng.2653> [published Online First: 2013/05/30].